4-1-2011

Characterization of theThreshold for NAD(P)H:quinone Oxidoreductase Activity in Intact Sulforaphane-treated Pulmonary Arterial Endothelial Cells

Robert D. Bongard
Medical College of Wisconsin

Gary S. Krenz
Marquette University, gary.krenz@marquette.edu

Adam J. Gastonguay
Medical College of Wisconsin

Carol L. Williams
Medical College of Wisconsin

Brian J. Lindemer
Medical College of Wisconsin

See next page for additional authors

Accepted version. *Free Radical Biology and Medicine*, Vol. 50, No. 8 (April 2011): 953-962. DOI.

Published in final edited form as:
Free Radic Biol Med. 2011 April 15; 50(8): . doi:10.1016/j.freeradbiomed.2011.01.009.

Characterization of the threshold for NAD(P)H:quinine oxidoreductase (NQO1) activity in intact sulforaphane treated pulmonary arterial endothelial cells

Robert D. Bongard[1], **Gary Krenz**[2], **Adam J. Gastonguay**[3], **Carol L. Williams**[3], **Brian J. Lindemer**[4], and **Marilyn P. Merker**[3,4,5]

[1]Department of Pulmonary Medicine, Medical College of Wisconsin, Milwaukee, WI 53295

[2]Departments of Mathematics, Statistics and Computer Science, Marquette University, Milwaukee, WI 53295

[3]Departments of Pharmacology and Toxicology, Medical College of Wisconsin, Milwaukee, WI 53295

[4]Department of Anesthesiology, Medical College of Wisconsin, Milwaukee, WI 53295

[5]Department of Zablocki VAMC, Milwaukee, WI 53295

Abstract

Treatment of bovine pulmonary arterial endothelial cells in culture with the phase II enzyme inducer sulforaphane (5 μM, 24 hrs; sulf-treated) increased cell lysate NQO1 activity by 5.7 ± 0.6 (mean ± SEM) fold, but intact cell NQO1 activity by only 2.8 ± 0.1 fold compared to control cells. To evaluate the hypothesis that the threshold for sulforaphane induced intact cell NQO1 activity reflects a limitation in the capacity to supply NADPH at a sufficient rate to drive all the induced NQO1 to its maximum activity, total KOH extractable pyridine nucleotides were measured in cells treated with duroquinone to stimulate maximal NQO1 activity. NQO1 activation increased $NADP^+$ in control and sulf-treated cells, with the effect more pronounced for the sulf-treated cells, in which the NADPH was also decreased. Glucose-6-phosphate dehydrogenase (G-6-PDH) inhibition partially blocked NQO1 activity in control and sulf-treated cells, but G-6-PDH overexpression via transient transfection with the human cDNA alleviated neither the restriction on intact sulf-treated cell NQO1 activity nor the impact on the NADPH/$NADP^+$ ratios. Intracellular ATP levels were not affected by NQO1 activation in control or sulf-treated cells. An increased dependence on extracellular glucose and a rightward shift in the K_m for extracellular glucose was observed in NQO1 stimulated sul-ftreated vs control cells. The data suggest that glucose transport in the sulftreated cells may be insufficient to support the increased metabolic demand for pentose phosphate pathway generated NADPH as an explanation for the NQO1 threshold.

Corresponding Author: Marilyn P Merker, PhD, Zablocki VAMC, 5000 W National Avenue, Department of Anesthesiology, Research Service 151, Milwaukee, Wisconsin 53295, 414-384-2000 x41394, FAX: 414-382-5374, mmerker@mcw.edu.

Keywords

lung; pulmonary endothelium; quinine; pyridine nucleotides; NAD(P)H; quinone oxidoreductase 1; mathematical model; glucose-6-phosphate dehydrogenase; sulforaphane

Introduction

NAD(P)H:quinone oxidoreductase (NQO1) is a two-electron quinone reductase present in a wide range of tissue and cell types including the pulmonary endothelium and other lung cells [1-7]. This predominately cytosolic (>90%) phase II enzyme catalyzes reduction of a wide spectrum of physiological, pharmacological and toxicological quinones and other redox active substances [1, 8, 9]. Depending on the chemical properties of the electron acceptor and the reaction product formed, NQO1 activity may mediate protective and anti-oxidant or toxic and pro-oxidant effects [1, 4, 8, 10-15].

Among the various roles in which NQO1 has been implicated, one is as a target for bioreductive activation of certain anticancer drugs and antioxidants and as a means of xenobiotic detoxification, wherein induction or genetic overexpression represent potential means to exploit these functions [12, 14, 16-20]. However, increases in NQO1 enzyme levels do not necessarily result in proportional increases in cellular effects (e.g., toxicity or antioxidant activity) of substances subject to NQO1 activation [12, 19, 21-28]. This phenomenon manifests itself as an upper threshold beyond which further increases in NQO1 levels do not result in enhanced effects of the NQO1-activated substrates [12, 19, 21-28].

In general, studies of the threshold effect have been limited by the lack of methodologies for quantifying intact cell NQO1 activity. Thus, whereas NQO1 activity is usually measured in cell lysates using a classical NQO1 enzyme assay, intact cell activity has largely been inferred from functional outcomes (e.g., toxicity or antioxidant protection) of NQO1 catalyzed activation of the compound under study. The only study we know of that included measurements of intact cell NQO1 activity was limited by the inability to obtain maximal activity using the chosen substrate [29]. The present study was motivated by the need to develop a quantitative basis for evaluating the threshold effect, wherein a further understanding of this phenomenon may suggest therapeutic strategies for increasing the efficacy of NQO1 targeted therapeutics.

In the present study, we sought to address the problem using an approach we developed for quantifying NQO1 activity in intact pulmonary arterial endothelial cells in culture. It involves the addition of the quinone, duroquinone (DQ), to the medium surrounding the cells and measuring the appearance rate of the two electron reduction product, durohydroquinone (DQH_2) using a secondary redox indicator. We have previously used this methodology to evaluate NQO1 kinetics, induction via hyperoxic exposure and electron donor preference in intact pulmonary arterial endothelial cells [2, 30, 31]. A variation of the method has also been used to evaluate NQO1 activity in the isolated perfused rodent lung [3].

Therefore, the overall objective of the present study was to quantify both intact cell and cell lysate NQO1 activity in control and sulforaphane induced (sulf-treated, 5 μM, 24 hrs) pulmonary arterial endothelial cells. The expectation was that NQO1 would be induced as a component of the overall phase II enzyme induction observed with sulforaphane treatment in other cell and organ systems, but not yet reported for pulmonary endothelial cells. Then, comparison of the fold differences in NQO1 activity in the intact cell and cell lysate assays would allow for determination of a threshold in the sulf-treated cells. If a threshold was observed, a second objective was to ask whether it could be explained by a limitation in the

capacity to generate sufficient electron donor to drive all the sulforaphane induced cell lysate NQO1 to its maximal intact cell rate. This concept was motivated by our previous studies implicating NADPH as the endogenous NQO1 electron donor in pulmonary arterial endothelial cells and by observations that, in general, quinone reduction appears to promote a drive to generate NADPH in other cell types [30, 32-34]. The approach was to evaluate the impact of NQO1 activation on cellular pyridine nucleotides, and the dependence of NQO1 activity on glucose-6-phosphate dehydrogenase (G-6-PDH) activity and extracellular glucose concentration.

Endothelial cells were selected for study because they are among the cell types that have relatively high NQO1 expression, which is perhaps not surprising given that they are in direct contact with blood-borne redox active xenobiotics, pharmacological and physiological quinones and other NQO1 substrates [7]. In this regard, pulmonary endothelial NQO1 may be of particular importance because of the large pulmonary endothelial surface area and position in the circulation. This property confers the ability to alter the redox status and disposition of redox active compounds during passage of the blood from the venous to the systemic arterial circulations [3, 35]. Sulforaphane was used as the phase II enzyme inducer because the lung is a key target organ of ingested dietary derived isothiocyanates, and there is intense interest in this class of compounds as cancer preventive, anti-inflammatory and oxidative stress protective agents in the lung, cardiovascular and other organ systems [20, 36-43]. In the vascular endothelium and lung, angiogenesis, inflammation, proliferation, carcinogenesis and other processes have been implicated as targets for manipulation by sulforaphane [38, 44-49]. From an experimental perspective, sulforaphane exposure also provides a model to evaluate the net effects of various phase II enzyme induced adaptive changes in cellular metabolism and redox function on intact cell NQO1 activity.

Materials and Methods

Materials

3-Potassium hexacyanoferrate (III) (hereafter referred to as $K_3Fe(CN)_6^{3-}$ or ferricyanide), 2,3,5,6-tetramethyl-1,4-benzoquinone (duroquinone, hereafter referred to as DQ), epiandrosterone (EPI), N-2-hydroxyethylpiperazine-N′-2-ethanesulfonic acid (HEPES), dicumarol, ATP and other chemicals, unless otherwise noted, were purchased from Sigma Chemical (St. Louis, MO). Sulforaphane was purchased from LKT Laboratories (St Paul, MN). Trypsin, penicillin-streptomycin, RPMI 1640 tissue culture medium, fetal calf serum, NuPAGE LDS sample buffer, 4-12% gradient Nu-PAGE Bis-Tris gels, MES-SDS running buffer and Lipofectamine 2000 were from Invitrogen (Grand Island, NY). Biosilon beads were from Nunc (Roskilde, Denmark). Pyridine nucleotide standards for HPLC were purchased from Boehringer Mannheim (Indianapolis, IN). Immunopure horseradish peroxidase and the SupersignalWest Pico Chemiluminescent substrate were from Thermo-Fisher Scientific (Rockford IL). The NQO1 inhibitor ES936 was the kind gift of Drs. David Siegel and David Ross (School of Pharmacy, University of Colorado Health Sciences Center, Denver, CO). The cDNA for human G-6-PDH was generously provided by Dr Margaret Briehl, University of Arizona [50].

Endothelial cell culture and sulforaphane treatment

Bovine pulmonary arterial endothelial cells were isolated from segments of calf pulmonary artery obtained from a local slaughterhouse, and cells between passages 4 and 20 were cultured to confluence on Biosilon microcarrier beads (mean diameter 230 μm; surface area 255 cm^2/gm beads) in magnetic stirrer bottles (Techne Inc., Burlington, N.J.) containing RPMI 1640 medium supplemented with 20% fetal calf serum, 100 U/ml penicillin, 100 μg/ml streptomycin and 30 mg/ml L-glutamine as previously described [2, 31]. The cells were

99.5% positive for DiO-acetylated-low density lipoprotein (Biomedical Technologies) uptake as measured by fluorescence activated cell sorting and exhibited cobblestone morphology as observed by phase contrast microscopy. Each passage of confluent cell cultures were separated into two groups, one of which was incubated in sulforaphane (5 μM), designated as sulf-treated, containing medium and one in medium alone for 24 hours before carrying out the described studies.

Protocol for measuring NQO1 activity in intact cells

DQ-mediated reduction of the cell membrane impermeant secondary electron acceptor, ferricyanide, was used to measure intact cell NQO1 activity, as previously described [2, 30, 31]. Approximately 0.2 - 0.3 ml packed volume of cell-coated beads were aliquoted from the stirred culture flasks into spectrophotometric cuvettes. After the cell-coated beads had settled, they were washed three consecutive times by resuspension in 3 ml of Hank's Balanced Salt Solution (HBSS) containing 10 mM HEPES, pH 7.4 and 5.5 mM glucose (HBSS/HEPES), allowing the beads to settle between each wash. The cell-coated beads were resuspended in 3 ml of HBSS/HEPES only (control) or HBSS/HEPES containing the various inhibitors or treatment conditions specified in the Results section and figure legends, and incubated with mixing on a Nutator mixer at 37°C for 10 min. Then the cell-coated beads were resuspended in 3 ml of fresh HBSS/HEPES containing 600 μM ferricyanide and DQ (at varying concentrations indicated in the text and figure legends) including the same treatments present during the 10-min pre-treatment incubation. The cell suspensions were mixed on a Nutator mixer at 37°C, and periodically the mixing was stopped, the cell-coated beads allowed to settle at the bottom of the spectrophotometric cuvettes out of the spectrophotometer light path, and the absorbance of ferricyanide in the medium measured at 421 nm using a Beckman Model DU 7400 spectrophotometer. The amount of the ferricyanide reduction product, ferrocyanide $\left(\mathrm{K_4Fe(CN)_6^{4-}}\right)$ in each sample was calculated from the decrease in ferricyanide absorbance at each time point (extinction coefficient 1.0 $\mathrm{mM^{-1} \cdot cm^{-1}}$). DQ-mediated ferricyanide reduction rates were determined from linear regression fits of the individual ferricyanide versus time curves [2]. The background rates of cell mediated ferricyanide reduction in the absence of DQ were subtracted from the individual rates obtained in their presence, normalized to the cell protein, and then combined to obtain mean rates. The DQ reduction rates were calculated as one-half the mean ferricyanide reduction rates. At the end of each experiment, the microcarrier beads were dried and weighed to determine the cell culture surface area for purposes of normalizing the data between experiments.

For measuring the dependence of intact cell NQO1 activity on the glucose concentration in the extracellular medium, the protocol was as described above except that wash solution was HBSS containing 10 mM HEPES and 2 mM pyruvate, pH 7.4, and either 0, 0.1, 0.3, 2.5 or 5.5 mM glucose. Following the washes, the cell coated beads were resuspended in the same medium in which they were washed, and with the DQ and ferricyanide as described above.

Measurement of DQ concentration in extracellular medium

Control or sulf-treated cells were incubated with 1 μM DQ for 30 min, the medium was removed from the cells and added to fresh control cells only. The DQ reduction rates of the two sets of control cells were measured as described above.

Cell lysate NQO1 and G-6-PDH activities

Cell lysates were prepared from cell-coated microcarrier beads by sonication (3 pulses of 15 sec each with the power output set to 6 watts using a Microson Ultasonic Cell Disrupter,

Farmington, NY) of ~ 0.2 ml of packed cell-coated beads on ice in 1 ml of 25 mM Tris-HCl buffer, pH 7.4.

NQO1 activity in cell lysates was determined using either the classical NQO1 electron acceptor 2,6-dichlorophenolindophenol (DCPIP) or DQ. DCPIP (50 μM) reduction was measured spectrophotometrically at 600 nm (extinction coefficient 21.0 $mM^{-1} \cdot cm^{-1}$) at 25°C following the addition of cell lysate fraction (~10 μg protein) to a reaction mixture containing 25 mM Tris-HCl, 0.02% bovine serum albumin, 0.01% Tween 20, 5 μM flavin adenine nucleotide (FAD) and 200 μM NADPH, pH 7.4, as previously described [2]. The difference between the reaction rates in the absence and presence of 10 μM dicumarol was used to calculate the NQO1 activity. When cell lysate NQO1 activity was measured using DQ, the buffer was the same as above with DQ (50 μM) substituted for the DCPIP and 45 μg/ml Immunopure horseradish peroxidase, 0.8 mM H_2O_2 and 0.15 mM NADPH added to the reaction mixture (total volume, 1 ml). The reaction was initiated by the addition of 50 μl of cell lysate and the decrease in NADPH absorbance over time at 25°C was measured spectrophotometrically at 340 nm and in the presence and absence of dicumarol. NADPH absorbance was used to calculate the NADPH oxidation rate using a molar extinction coefficient of 6.22 $mM^{-1} \cdot cm^{-1}$. The difference between the reaction rates in the absence and presence of 10 μM dicumarol was used to calculate the NQO1 activity.

G-6-PDH activity was determined by measuring the rate of NADPH generation from $NADP^+$ spectrophotometrically at 340 nm (extinction coefficient 6.22 mM^{-1} (x000B7) cm^{-1}) at 25°C following the addition of the cell lysate fraction (~75 μg protein) to a reaction mixture containing 55mM Tris-HCl (pH 7.4), 3.3 mM $MgCl_2 \cdot 6H_2O$, 3.3 mM glucose-6-phosphate and 2.0 mM $NADP^+$[51].

The reaction rates were normalized to the cell lysate protein as measured by the Bio-Rad or BCA protein assays.

Immunoblotting for NQO1

Portions of control and sulf-treated cell lysates, prepared as described above, or purified recombinant human NQO1 (hrNQO1, 0.5 ng protein) were subjected to SDS-PAGE electrophoresis using Invitrogen's NuPAGE LDS sample buffer, 4-12% gradient Nu-PAGE Bis-Tris gels and MES-SDS running buffer, as we previously described [3, 6]. The amounts of cell lysate protein loaded onto the gels is described in the Figure 3 legend. The separated proteins were transferred to a nitrocellulose membrane, and incubated for 1 h in Tris-buffered saline containing 0.1% Tween 20 and 2% bovine serum albumin, the latter as a blocking agent. The membrane was then incubated sequentially in a 1:1000 dilution of primary antibody (polyclonal goat anti-rabbit NQO1), a 1:20,000 dilution of secondary antibody (rabbit anti-goat IgG-horseradish peroxidase conjugate) and the Supersignal West Pico Chemiluminescent substrate. The image was captured and band intensities quantified using a Kodak IS 2000 MMT ImageStation and Image Station software. NQO1 protein on the blots was quantified using the hrNQO1 as a standard under conditions in which the band intensities vs μg protein loaded relationship was in the linear range of intensities. The NQO1 protein amounts were normalized to total cell lysate protein loaded onto the lanes to obtain the amount of NQO1 protein per mg cell lysate protein.

Pyridine nucleotide and ATP high performance liquid chromatography (HPLC)

Cell-coated beads were washed free of growth medium as described above. The washed cell-coated beads were aliquoted into conical bottom centrifuge tubes and incubated in HBSS/HEPES without or with DQ for 15 min at 37°C on a Nutator. Following the incubation, the cell-coated beads were allowed to settle, the experimental medium was

removed, and the pyridine nucleotides extracted with ice cold KOH prior to HPLC as previously described [30]. Pyridine nucleotide and ATP levels were normalized to cm^2 cell culture surface area.

Transfection with cDNA for G-6-PDH

G-6-PDH overexpressing bovine pulmonary arterial endothelial cells were obtained by transient transfection with a cDNA for human G-6-PDH, kindly provided by Dr Margaret Briehl, University of Arizona [50]. The G-6-PDH cDNA was subcloned into the pcDNA3.1 vector and the sequence confirmed using PCR. Cells were transfected using Lipofectamine 2000 according to the manufacturer's protocol. Successful transfection was confirmed 2 days later by enzyme assay for G-6-PDH in cell lysates. As controls for the G-6-PDH transfected cells, cells were treated with Lipofectamine 2000 in the absence of the vector (mock transfected). After 2 days, cells were further incubated in cell medium with or without sulforaphane (5 μM) for 24 hours.

Additional measurements

As a measure of cell viability, lactate dehydrogenase (LDH) activity in the treatment medium and in the cells at the end of each experimental protocol was determined, and the % total LDH release calculated, as previously described [2]. The total cell LDH activities for control and sulforaphane cells were 3.44 ± 0.08 and 3.58 ± 0.05 (mean ± SEM) units per μg cell protein, with no significant difference between the activities, or under the different experimental conditions ($p>0.05$, t-test). The % LDH release did not exceed 1.58 ± 0.37% of total cell LDH for all the studies combined, with no significant differences between conditions ($p>0.05$, ANOVA). To normalize the data for comparisons between studies, the protein content of the cells in each experiment was measured using the BioRad or Pierce BCA protein assays, previously described for the BioRad assay in [2]. One cm^2 of cell surface area of confluent control or sulf-treated endothelial cells cultured on the Biosilon microcarrier beads contained 25.5 ± 0.3 μg (mean ± SEM) protein.

Statistical analysis

Data are expressed as mean ± standard error (mean ± SEM). Statistical analysis was performed using SigmaStat (Jandel Scientific, San Rafael, CA). Differences between groups were evaluated using the *t*-test, or ANOVA followed by Tukey test.

Results

Figure 1 illustrates the approach used to measure NQO1 activity in intact pulmonary arterial endothelial cells, which involves the addition of DQ and ferricyanide to the medium surrounding the cells, as previously described [2, 30, 31]. The method relies on the fact that both DQ and its hydroquinone (DQH_2) are freely membrane permeant, whereas both ferricyanide and its reduction product, ferrocyanide, are cell membrane impermeant [2, 30, 31]. DQ enters the cells and is reduced to DQH_2 via NQO1 at the expense of intracellular NADPH [30]. Then, the DQH_2 leaves the cell where it is virtually instantaneously reduced by the ferricyanide in the extracellular medium. Under these reaction conditions, DQ is continually regenerated in the extracellular medium, maintaining steady state DQ reduction kinetics as reflected by the zero order ferricyanide vs time progress curves. The ferricyanide reduction remains zero order until the ferricyanide is exhausted, as expected of a secondary electron acceptor that is essentially irreversibly reduced and does not influence the primary reduction rate [2, 30, 31]. In addition the ferricyanide concentration is sufficient to act as an extracellular sink for intracellular NQO1 generated DQH_2. Taken together, the zero order ferricyanide reduction rates provide measurements of intracellular NQO1 activity [2, 30, 31].

Figure 1 shows the DQ-mediated ferricyanide reduction rates versus time for control (Figure 1A) and sulf-treated (Figure 1B) cells for a range of DQ concentrations. Also shown is that ferricyanide alone is not substantially reduced in the absence of DQ. Figures 1A and B also show that the competitive NQO1 inhibitor, dicumarol, blocks ferricyanide reduction in the presence of the highest DQ concentration used, 50 μM, for both control and sulf-treated cells.

Figure 2 shows the dependence of the DQ reduction rates, calculated from the data in Figure 1, on DQ concentration (0 - 50 μM) for control and sulf-treated cells. The reduction rates increased in a concentration-dependent manner over the range of 1-10 μM DQ, reaching a maximum for both cell conditions at ∼10 μM DQ (Figure 2). At the maximal rates, the apparent NQO1 activity was about ∼3 fold higher for the sulf-treated than control cells. However, at DQ concentrations of 1 and 3 μM, the difference between the reduction rates for the control and sulf-treated cells was further diminished. One possible explanation for the observations at low DQ concentrations is a sulforaphane induced increase in DQ conjugating enzymes, which could decrease the free DQ concentration and hence the apparent DQ reduction rate. However, there was no detectable difference between the DQ concentrations in the medium of control and sulf-treated cells incubated with 1 μM DQ under the study conditions ($p > 0.05$; $n = 3$; data not shown).

Figure 2 also shows that dicumarol blocked DQ reduction at all DQ concentrations studied for both control and sulf-treated cells. This is consistent with the data shown for dicumarol with 50 μM DQ in Figures 1A and B. Figure 2 additionally shows the inhibitory effect of the irreversible NQO1 inhibitor, ES936, on DQ reduction for the sulf-treated cells, as we have previously demonstrated for control cells [30, 31]. The nearly complete inhibitory effect of both NQO1 inhibitors is consistent with the DQ reduction rate measurement as a selective NQO1 activity indicator in intact pulmonary arterial endothelial cells. All further studies were carried out at 50 μM DQ to achieve maximal intact cell NQO1 activity.

Figure 3 shows immunoblots for NQO1 protein in control and sulf-treated treated cells, wherein the blots in Figure 3A were loaded with equal amounts of control and sulf-treated cell lysate protein (20 μg) and those in Figure 3B with 10 times more control than sulf-treated cell lysate protein, that is, 20 vs 2 μg, respectively. Figure 3C shows the total NQO1 on the blots calculated from the lane intensities in Figure 3B, and Figure 3D shows that there was 7 times more NQO1 protein per mg total cell protein for the sulf-treated vs control cells.

The maximal intact cell NQO1 activity, measured as DQ-mediated ferricyanide reduction, was 2.8 ± 0.1 (mean ± SEM) fold higher in sulf-treated than control cells (Figure 4A). The sulf-treated cell lysate activity, measured using either DCPIP or DQ as the electron acceptor, was 5.7 ± 0.6 (mean ± SEM) or 5.1 ± 0.5 (mean ± SEM) fold higher, respectively, than the control cell lysate activity (Figure 4B). There was no significant difference between the fold increases observed with the two electron acceptors ($p > 0.05$, t-test). Figure 4C shows the relationship between the sulforaphane induced fold increase in cell intact cell NQO1 activity vs the fold increase in cell lysate NQO1 activity for all 20 pairs of control vs sulf-treated cells in Figures 4A and B. The sulforaphane induced increase in intact cell NQO1 activity was capped at 3.6 fold even when the increase in cell lysate activity ranged as high as 11 fold.

The apparent limitation on intact sulf-treated cell NQO1 activity is further emphasized by the observation that when the cells were subjected to H_2O_2 as an oxidative stress, the maximal intact cell NQO1 activity was depressed in the sulf-treated but not control cells (Figure 5). The depression was not attributable to any direct effect of H_2O_2 on intrinsic NQO1 activity insofar as there was no detectable difference in NQO1 activities in cell

lysates from control and H_2O_2 treated cells ($p>0.05$, t-test, data not shown). There was also no difference in the G-6-PDH activities in lysates from control and H_2O_2 treated cells ($p>0.05$, t-test, data not shown), and no decrease in cell viability (% LDH release) due to H_2O_2 treatment ($p>0.05$, t-test, data not shown).

Since one mechanism by which H_2O_2 exerts an oxidative stress in endothelial cells is to increase the demand on the pentose phosphate pathway, we sought more direct evidence for involvement of this pathway in the intact cell NQO1 activity [52, 53]. Figure 6 shows that the G-6-PDH inhibitor EPI depressed intact control and sulf-treated cell NQO1 activity. The EPI effect on the control cells was consistent with previous studies [30].

To evaluate the impact of NQO1 stimulation on pyridine nucleotide redox status, total cell KOH extractable NAD^+, $NADP^+$, NADH and NADPH were measured in the absence and presence of 50 μM DQ. In both the control and sulf-treated cells, DQ increased $NADP^+$ and in the sulf-treated cells, a decrease in NADPH was also detected (Figures 7 A and C). The NADPH/$NADP^+$ ratios decreased for both the control and sulf-treated cells, wherein the decrease was more pronounced for the sulf-treated cells (Figure 7E). Although the sulf-treated cells also had lower NAD^+ than the control cells when DQ was present, there was no detectable effect on NADH levels or the NADH/NAD^+ redox pair in control or sulf-treated cells (Figure 7B, D and F). The observations for the control cells were consistent with our previous study revealing a tighter coupling of intact cell NQO1 activity to the intracellular NADPH/$NADP^+$ than the NADH/NAD^+ redox pair, thereby implicating NADPH as the endogenous NQO1 electron donor [30].

Although $NADP^+$ was previously ruled out as an NQO1 inhibitor in studies of isolated rat liver cytosol NQO1, the more elevated $NADP^+$ in NQO1 activated sulf-treated as compared to control cells raised the question of $NADP^+$ as a potential NQO1 inhibitor [54]. When cell lysate NQO1 assays were carried out with the usual 0.20 mM NADPH in the absence or presence of $NADP^+$ (0.06, 0.20, 0.60 or 2.00 mM), there was no detectable inhibition of sulf-treated cell lysate NQO1 activity at any $NADP^+$ concentration studied ($p < 0.05$; n =7 different cell populations each $NADP^+$ concentration; data not shown). There was also no detectable inhibition of control cell lysate NQO1 activity at 0.06, 0.20 or 0.60 mM $NADP^+$ ($p > 0.05$; n =7 different cell populations each $NADP^+$ concentration; data not shown); a 23 ± 3 (mean ± SEM) % inhibition of control cell lysate activity was observed only at the highest $NADP^+$ concentration studied (2.00 mM; $p < 0.05$; n = 7 different cell populations; data not shown).

The Figures 5-7 data suggested that overexpressing G-6-PDH in the sulf-treated cells might represent a means to overcome the restriction on the induced NQO1 activity. Figure 8A shows that the baseline G-6-PDH activities in the control and sulf-treated cell lysates were not detectably different and that transient transfection with a cDNA for human G-6-PDH increased cell lysate G-6-PDH activity to the same extent in both control and sulf-treated cells (Figure 8A). There was no detectable effect of G-6-PDH overexpression on cell lysate NQO1 activity in control or sulf-treated cells, and therefore no compensatory effects of the transfection on intrinsic NQO1 activity (Figure 8B). However, G-6-PDH overexpression did not facilitate intact cell NQO1 activity in either control or sulf-treated cells (Figure 8C).

Figure 9 shows that G-6-PDH overexpression also did not mitigate against the DQ induced effects on $NADP^+$, NADPH or the NADPH/$NADP^+$ ratios seen in the absence of overexpression. That is, the Figure 9 data qualitatively reproduce the patterns seen in the NADP(H) data (Figure 7A, C, E) in the absence of G6PDH overexpression.

Since the threshold for intact sulf-cell NQO1 activity could not be attributed to limitations in G-6-PDH activity, and intracellular ATP was not detectably altered in the presence of DQ

(50 μM) to activate NQO1 in either control or sulf-treated cells (t-test, $p>0.05$; data not shown), we asked whether more proximal processes contributing to intact cell NADPH regeneration capacity and NQO1 driven DQ reduction, e.g., glucose transport, were implicated. One means of identifying mechanisms involved in control of glucose utilization in neuronal and other cell types has been to evaluate the dependence of intracellular glucose-6-phosphate generation on the extracellular glucose concentration [55].

Figure 10 shows the dependence of intact control and sulf-treated cell NQO1 activities on the glucose concentration in the extracellular medium. The sulf-treated cell NQO1 activity was dramatically more sensitive to limiting the extracellular glucose concentration. To emphasize this point, the difference between the control cell NQO1 activities at 0 and 5.5 mM glucose comprised a total of only 3.3 nmol DQ reduced per min per mg cell protein; this difference was an order of magnitude higher for the sulf-treated cells (34.2 nmol DQ reduced/min/mg cell protein). Furthermore, the apparent K_m for extracellular glucose was shifted to the right for the sulf-treated as compared to control cells.

The studies in Figures 1 – 9 were all carried out at 5.5 mM glucose. Additional studies in which extracellular glucose was increased to 11 or 22 mM resulted in no further increase in NQO1 activity beyond that observed with 5.5 mM glucose for either control or sulf-treated cells ($p > 0.05$; data not shown).

Discussion

The study showed that exposure of pulmonary arterial endothelial cells to sulforaphane (5 μM, 24 hrs) increased cell lysate NQO1 activity and protein levels, wherein the quantitative increases were reasonably consistent with each other. Furthermore, the study made use of an intact cell NQO1 activity assay, to our knowledge the first such assay to provide quantitative information at maximal NQO1 activities, to show that intact cell NQO1 activity was also elevated in sulf-treated cells. However, the increase in intact cell activity did not increase to the extent predicted from the cell lysate activity measurements. Importantly, the magnitude of this restriction was independent of whether the cell lysate assay was carried out using the classical NQO1 electron acceptor DCPIP or the electron acceptor used in the intact cell assay, DQ. The implication is that the threshold phenomenon in the sulf-treated pulmonary endothelial cells cannot be assigned to a difference in electron acceptor preference of any induced NQO1 isoform, should it exist in the pulmonary arterial endothelial cells. Thus, our study provides the first direct, quantitative evidence of an NQO1 activity threshold in pulmonary endothelial or any other intact cells.

The availability of a quantitative intact cell NQO1 activity assay was paramount for evaluation of a threshold effect. The assay we developed is such a powerful and unique tool because it was designed to optimize the specificity for NQO1 and because it provides rates for the maximal intact cell NQO1 activity. The specificity is revealed by observations that the vast majority of DQ reduction at all DQ concentrations studied is sensitive to two mechanistically different NQO1 inhibitors, the competitive inhibitor dicumarol and the irreversible inhibitor ES936 (present study and [31]). Secondly, ferricyanide acts as a sink for the cell generated DQH_2, minimizing its intracellular re-oxidation via mitochondrial electron transport complex III or its conjugation via other phase II enzymes [31]. Finally, both DQ and DQH_2 are relatively stable as compared to other quinone-hydroquinone pairs with regard to autoxidation-comproportionation or redox cycling [31]. Thus, under the experimental conditions described, the dominating reactions involving DQ and DQH_2 are reduction via NQO1 and re-oxidation via ferricyanide, respectively. The specificity of the DQ-ferricyanide assay system for intact cell NQO1 activity helped to ensure that regardless of whether sulforaphane affected expression of other quinone reductases and/or other redox

and metabolic processes, the potential for such alterations to influence the measurement were minimized [38].

The magnitude of the NQO1 activity threshold is revealed by the Figure 2 and 4 studies. In Figure 2, the dotted line illustrates the control cell DQ reduction rates multiplied by 5.7, the increase predicted if the intact sulf-treated cell activity increased in direct proportion to the cell lysate activity. Instead, the maximum sulf-treated cell NQO1 activities were only about half that predicted from the cell lysate activities. Although the remaining studies focused primarily on the maximal NQO1 activities, using 50 μM DQ, it is intriguing to note that at DQ concentrations that stimulate only sub-maximal activation (below 10 μM), the threshold is exaggerated to the extent that there is little detectable difference between the control and sulf-treated cells. These observations emphasize the importance of taking electron acceptor concentration and extent of NQO1 activation into consideration when evaluating a possible threshold for intact cell or organ NQO1 activity.

In Figure 4, the magnitude of the threshold is revealed by the relationship between the fold changes in cell lysate and intact cell NQO1 activities. All of the symbols lie below the line of identity, included to emphasize the point that although the cell lysate NQO1 activity increased up to 11 fold for the individual pairs of control and sulf-treated cell populations studied, the increase in intact cell activity was restricted to at most a 3.6 fold increase for any given pair. That the range achieved in the fold increases for the cell lysate activities is much greater than the range that can be attained for the intact cell activities is a manifestation of a restriction, or threshold, for intact cell NQO1 activity.

Previous explanations for the threshold effect have included, in cases where the measurement consisted of a toxicity index, saturation of the lesion being measured (e.g., formation of cytotoxic DNA crosslinks), limitation in substrate uptake or metabolism and restriction in electron donor supply [19, 24, 26]. In the present studies, lesion saturation is not pertinent since we measured NQO1 activity itself rather than a functional consequence thereof. A limitation in substrate uptake or metabolism is also not relevant since the DQ concentration vs intact cell NQO1 activity measurements included DQ concentrations that achieved maximal activity. DQ and DQH_2 cell membrane permeability are virtually unlimited and nearly all the DQ (in the absence or presence of ferricyanide) initially added to the cells can be accounted for in the extracellular medium or bound to the experimental plasticware at the end of the 30 min incubations with the cells ([31] and present study).

Several observations suggested that a limitation in the capacity to regenerate NADPH could contribute to explaining the sulf-treated cell NQO1 threshold. NQO1 activation increased cellular $NADP^+$ levels and decreased the NADPH/$NADP^+$ ratios in both control and sulf-treated cells. The effects were more pronounced in sulf-treated cells, for which a depression in NADPH was additionally detected. One interpretation is that NQO1 activation placed a higher demand on the cells for NADPH in the sulf-treated cells because of the induced NQO1. That the effect was more dramatically revealed in the $NADP^+$ and NADPH/$NADP^+$ ratios than in the NADPH itself might be explained by first noting that the measurements were of total KOH extractable pyridine nucleotides. Whereas the presumption is that the total cell pyridine nucleotide levels reflect changes within the cytosol when cytosolic processes are targeted, the measurement does not take into account intracellular compartmentalization or macromolecular binding of coenzymes [56, 57]. Thus, the magnitude of the impact on the NADPH pool supplying the NQO1 may be masked in the total cell measurement. Secondly, the zero order ferricyanide vs time progress curves in Figure 1 imply steady state DQ reduction kinetics and hence a steady state NADPH regeneration rate throughout the reaction time course [31]. The implication is that new steady state pyridine nucleotide levels are attained upon addition of DQ and ferricyanide to

the cells, with the change from control occurring too rapidly to be detected on the time course of the measurements.

Cells challenged with quinones have been reported to mobilize cytosolic and mitochondrial sources of pyridine nucleotides via a network of metabolic processes including interconversion reactions in an attempt to maintain NADPH levels [32-34]. For example, in colon epithelial cells, quinone treatment increased $NADP^+$ at the expense of NAD^+, consistent with our observations [32]. Whereas the observation that EPI depresses intact cell NQO1 activity implicates the pentose phosphate pathway as a key source of NADPH in pulmonary endothelial cells, the EPI-insensitive NQO1 activity suggests the potential for contributions to cytosolic NADPH from such alternate pathways, e.g., cytosolic isocitrate dehydrogenase and/or malic enzyme. While it is also possible that DQ redox cycling contributed to changes in NADPH/$NADP^+$ balance, DQ is relatively inactive in this regard as compared to other redox cycling quinones, and if anything, we would anticipate the sulf-treated cells to be more resistant to such depletion due to induction of an array of phase II antioxidant enzymes.

The dampening effect of H_2O_2 on sulf-treated but not control cell activity further suggested that the threshold might be attributable to a limitation in the capacity to supply NADPH. The effect of H_2O_2 was not attributable to NQO1 or G-6-PDH inactivation, implying an indirect mechanism. Several known effects of H_2O_2 involve an impact on NADPH, for example, H_2O_2 increases the demand on the endothelial cell pentose phosphate pathway as a means to provision the glutathione redox cycle with NADPH [52, 53]. Thus, we suggest that when both H_2O_2 and DQ are present, the glutathione redox cycle and NQO1 are in competition for NADPH. The competition is intensified in the sulf-treated cells due to the induced NQO1 and NQO1 activity is compromised, unmasking a threshold for the NADPH regeneration capacity. Other effects of H_2O_2 in vascular endothelial and other cell types that could compromise NADPH include activation of poly(ADP- ribose) polymerase 1 (PARP-1), which depletes ATP and inhibition of glucose dependent ATP synthesis [58-60].

Interpreting the NQO1 mediated decrease in the sulf-treated cell NADPH/$NADP^+$ ratio as a reflection of a limitation in NADPH regeneration capacity suggested G-6-PDH overexpression as a possible means for overcoming this restriction. This approach was motivated by observations that transfection with recombinant adenovirus encoding G-6-PDH cDNA enhanced vascular endothelial cell eNOS activity, nitric oxide production and cell proliferation and angiogenesis, presumably via increased capacity to provide NADPH [61]. In addition, in vascular endothelial, NIH 3T3 and HeLa cells, G-6-PDH overexpression improved resistance to oxidative stress, attributed to enhanced NADPH for maintenance of glutathione redox cycle [62-64]. Nevertheless, G-6-PDH overexpression did not increase maximal NQO1 activity in either the control or sulf-treated cells. A limitation in free $NADP^+$, which at least in Ehrlich ascites cells is one-third the K_m of G-6-PDH for $NADP^+$, has been suggested to be a key regulatory factor in intact cell G-6-PDH activity [65]. Thus, the extent to which G-P-PDH overexpression provides a means to drive NADPH regeneration may depend on a variety of factors, e.g., the extent of the metabolic demand for NADPH and the total available NADPH+$NADP^+$ pool.

The intact sulf-treated cell NQO1 activity was more sensitive than the control cell activity to extracellular glucose concentration. The sensitivity was manifested in the larger fraction of NQO1 activity that relied on the presence of extracellular glucose and the pronounced concentration dependence of the activity, across the entire 0 – 5.5 mM range of glucose concentrations studied. The increased glucose sensitivity together with the pyridine nucleotide data suggest that the induced NQO1 in the sulf-treated cells drives an increased demand for pentose phosphate pathway generated NADPH, consistent with the demand

imposed in other cell types by quinones [32-34]. This would be transmitted as an increased demand for glucose-6-phosphate, relief of hexokinase product inhibition and stimulation of glucose phosphorylation and transport. Since ATP was not depressed when NQO1 was activated, glucose transport may be implicated as a factor limiting pentose phosphate pathway catalyzed NADPH generation in the sulf-treated cells. A shift in metabolic control from hexokinase to glucose transport in the sulf-treated cells could explain the higher K_m for both glucose (Figure 10) and DQ (Figure 2). This interpretation is suggested by studies in neurons and other cell types in which the rate limiting step in glucose-6-phosphate generation is inferred based on a presumptive difference in the K_m for extracellular glucose for glucose transport vs hexokinase activity [55]. However, the degree to which the control point in glucose utilization under conditions of metabolic stress can be attributed to glucose transport, hexokinase or other factors is a hotly debated topic, even in skeletal muscle where it has been so extensively studied [66]. To the extent that intact cell NQO1-catalyzed DQ reduction rates reflect not only processes regulating glucose-6-phosphate production, but also downstream G-6-PDH activity, extends the candidate field for limiting factors, eg., to free $NADP^+$[65].

The advantage of using an inducer to study the impact on functional intact cell NQO1 activity has translational relevance insofar as isothiocyanates are dietary derived substances that promote anti-inflammatory, anti-carcinogenic, antioxidant function [20, 36-42]. This sulforaphane effect to induce NQO1 in the pulmonary endothelial cells is consistent with its known function as a potent phase II enzyme inducer in human microvascular and umbilical vein endothelial cells, various lung cells, and other cells and organs [37-41, 49]. The sulforaphane concentration used was in the present study was physiologically relevant insofar as it was in the range of plasma concentrations achieved in studies of humans consuming broccoli, a rich source of isothiocyanates, and lower than that measured in rat plasma after oral dosing with sulforaphane at levels sufficient to induce phase II liver enzymes [67, 68]. It was also reasonably close to concentrations that alter signal transduction and other processes in vascular endothelial cells and induce phase II enzymes, including NQO1, in human EAhy926 endothelial cells and rat lung slices [38, 40, 44-47].

Our studies provide evidence that the NQO1 threshold may be at least in part attributed to a limitation in the ability to regenerate NADPH at a sufficient rate to drive all the induced NQO1 activity to its maximum rate. The dearth of studies of pulmonary endothelial bioenergetics and pathways of pyridine nucleotide metabolism underscores the necessity for additional studies in this area to promote understanding of responses to increased metabolic demand in lung injury and repair. This is perhaps especially important with regard to the pulmonary endothelium, which is exquisitely sensitive to oxidative stresses and in direct contact with blood borne xenobiotics and toxins. Our studies provide the groundwork for eventual evaluation of the utility of isothiocyanates and other phase II enzyme inducers as a means to optimize the therapeutic efficacy of NQO1 targeted anticancer drugs and antioxidants in the pulmonary endothelium, lung and other cell types and organ systems.

Acknowledgments

Supported by NHLBI HL-65537 (M.P.M.), GM-069700 (C.L.W.) and the Dept of Veterans Affairs (M.P.M.). We are grateful to Dr Margaret Briehl, University of Arizona, for providing the cDNA for human G-6-PDH [50], and to Drs David Ross and David Siegel, University of Colorado, for supplying the ES936. We also thank Dr James May, Vanderbilt University, for helpful discussion.

Reference List

1. Cadenas E. Antioxidant and prooxidant functions of DT-diaphorase in quinone metabolism. Biochem Pharmacol. 1995; 49:127–40. [Review] [140 refs]. [PubMed: 7530954]

2. Merker MP, Audi SH, Bongard RD, Lindemer BJ, Krenz GS. Influence of pulmonary arterial endothelial cells on quinone redox status: effect of hyperoxia induced increase in NAD(P)H quinone oxidoreductase 1 (NQO1). Am J Physiol Lung Cell Mol Physiol. 2006; 289:788–97.

3. Audi SH, Bongard RD, Krenz GS, Rickaby DA, Haworth ST, Eisenhauer J, et al. Effect of chronic hyperoxic exposure on duroquinone reduction in adult rat lungs. Am J Physiol Lung Cell Mol Physiol. 2005; 289:788–L797.

4. Ross D. Quinone reductases multitasking in the metabolic world. Drug Metab Rev. 2004; 36:639–54. [PubMed: 15554240]

5. Siegel D, Franklin WA, Ross D. Immunohistochemical detection of NAD(P)H:quinone oxidoreductase in human lung and lung tumors. Clin Cancer Res. 1998; 4:2065–70. [PubMed: 9748120]

6. Audi SH, Bongard RD, Dawson CA, Siegel D, Roerig DL, Merker MP. Duroquinone reduction during passage through the pulmonary circulation. Am J Physiol Lung Cell Mol Physiol. 2003; 285:1116–L1131.

7. Siegel D, Ross D. Immunodetection of NAD(P)H:quinone oxidoreductase 1 (NQO1) in human tissues. Free Radic Biol Med. 2000; 29:246–53. [PubMed: 11035253]

8. Ross D, Kepa JK, Winski SL, Beall HD, Anwar A, Siegel D. NAD(P)H:quinone oxidoreductase 1 (NQO1): chemoprotection, bioactivation, gene regulation and genetic polymorphisms. Chem Biol Interact. 2000; 129:77–97. [PubMed: 11154736]

9. O'Brien PJ. Molecular mechanisms of quinone cytotoxicity. Chem Biol Interact. 1991; 80:1–41. [PubMed: 1913977]

10. Colucci MA, Moody CJ, Couch GD. Natural and synthetic quinones and their reduction by the quinone reductase enzyme NQO1: from synthetic organic chemistry to compounds with anticancer potential. Org Biomol Chem. 2008; 6:637–56. [PubMed: 18264564]

11. Rooseboom M, Commandeur JNM, Vermeulen NPE. Enzyme-Catalyzed Activation of Anticancer Prodrugs. Pharmacol Rev. 2004; 56:53–102. [PubMed: 15001663]

12. Siegel D, Bolton EM, Burr JA, Liebler DC, Ross D. The reduction of alpha-tocopherolquinone by human NAD(P)H: quinone oxidoreductase: the role of alpha-tocopherolhydroquinone as a cellular antioxidant. Mol Pharmacol. 1997; 52:300–5. [PubMed: 9271353]

13. Bello RI, Kagan VE, Tyurin V, Navarro F, Alcain FJ, Villalba JM. Regeneration of lipophilic antioxidants by NAD(P)H:quinone oxidoreductase 1. Protoplasma. 2003; 221:129–35. [PubMed: 12768350]

14. Danson S, Ward TH, Butler J, Ranson M. DT-diaphorase: a target for new anticancer drugs. Cancer Treat Rev. 2004; 30:437–49. [PubMed: 15245776]

15. Guo W, Reigan P, Siegel D, Zirrolli J, Gustafson D, Ross D. The bioreduction of a series of benzoquinone ansamycins by NAD(P)H:quinone oxidoreductase 1 to more potent heat shock protein 90 inhibitors, the hydroquinone ansamycins. Mol Pharmacol. 2006; 70:1194–203. [PubMed: 16825487]

16. Lewis AM, Ough M, Hinkhouse MM, Tsao MS, Oberley LW, Cullen JJ. Targeting NAD(P)H:quinone oxidoreductase (NQO1) in pancreatic cancer. Mol Carcinog. 2005; 43:215–24. [PubMed: 16003741]

17. Park HJ, Choi EK, Choi J, Ahn KJ, Kim EJ, Ji IM, et al. Heat-induced up-regulation of NAD(P)H:quinone oxidoreductase potentiates anticancer effects of β-lapachone. Clin Cancer Res. 2005; 11:8866–71. [PubMed: 16361576]

18. Wang X, Doherty GP, Leith MK, Curphey TJ, Begleiter A. Enhanced cytotoxicity of mitomycin C in human tumour cells with inducers of DT-diaphorase. Br J Cancer. 1999; 80:1223–30. [PubMed: 10376975]

19. Seow HA, Penketh PG, Belcourt MF, Tomasz M, Rockwell S, Sartorelli AC. Nuclear overexpression of NAD(P)H:quinone oxidoreductase 1 in Chinese hamster ovary cells increases the cytotoxicity of mitomycin C under aerobic and hypoxic conditions. J Biol Chem. 2004; 279:31606–12. [PubMed: 15155746]

20. Tan XL, Spivack SD. Dietary chemoprevention strategies for induction of phase II xenobiotic-metabolizing enzymes in lung carcinogenesis: A review. Lung Cancer. 2009; 65:129–37. [PubMed: 19185948]

21. de Haan LH, Pot GK, Aarts JM, Rietjens IM, Alink GM. In vivo relevance of two critical levels for NAD(P)H:quinone oxidoreductase (NQO1)-mediated cellular protection against electrophile toxicity found in vitro. Toxicol In Vitro. 2005; 20:594–600. [PubMed: 16314070]
22. De Haan LHJ, Boerboom AMJF, Rietjens IMCM, van Capelle D, De Ruijter AJM, Jaiswal AK, et al. A physiological threshold for protection against menadione toxicity by human NAD(P)H: quinone oxidoreductase (NQO1) in Chinese hamster ovary (CHO) cells. Biochem Pharmacol. 2002; 64:1597–603. [PubMed: 12429349]
23. Gliszczynska-Swiglo A, vander WH, de Haan L, Tyrakowska B, Aarts JM, Rietjens IM. The role of quinone reductase (NQO1) and quinone chemistry in quercetin cytotoxicity. Toxicol In Vitro. 2003; 17:423–31. [PubMed: 12849725]
24. Winski SL, Swann E, Hargreaves RH, Dehn DL, Butler J, Moody CJ, et al. Relationship between NAD(P)H:quinone oxidoreductase 1 (NQO1) levels in a series of stably transfected cell lines and susceptibility to antitumor quinones. Biochem Pharmacol. 2001; 12:1509–16. [PubMed: 11377380]
25. Gustafson DL, Beall HD, Bolton EM, Ross D, Waldren CA. Expression of human NAD(P)H: quinone oxidoreductase (DT-diaphorase) in Chinese hamster ovary cells: effect on the toxicity of antitumor quinones. Mol Pharmacol. 1996; 50:728–35. [PubMed: 8863816]
26. Mikami K, Naito M, Tomida A, Yamada M, Sirakusa T, Tsuruo T. DT-diaphorase as a critical determinant of sensitivity to mitomycin C in human colon and gastric carcinoma cell lines. Cancer Res. 1996; 56:2823–6. [PubMed: 8665520]
27. Begleiter, A.; Fourie, J. Induction of NQO1 in Cancer Cells. In: Helmut, Sies; Lester, Packer, editors. Methods in Enzymology Quinones and Quinone Enzymes, Part B. Academic Press; 2004. p. 320-51.
28. Digby T, Leith MK, Thliveris JA, Begleiter A. Effect of NQO1 induction on the antitumor activity of RH1 in human tumors in vitro and in vivo. Cancer Chemother Pharmacol. 2005; 56:307–16. [PubMed: 15877230]
29. Lee YY, Westphal AH, de Haan LH, Aarts JM, Rietjens IM, van Berkel WJ. Human NAD(P)H:quinone oxidoreductase inhibition by flavonoids in living cells. Free Radic Biol Med. 2005; 39:257–65. [PubMed: 15964517]
30. Bongard RD, Lindemer BJ, Krenz GS, Merker MP. Preferential utilization of NADPH as the endogenous electron donor for NAD(P)H:quinone oxidoreductase 1 (NQO1) in intact pulmonary arterial endothelial cells. Free Radic Biol Med. 2009; 46:25–32. [PubMed: 18848878]
31. Merker MP, Bongard RD, Krenz GS, Zhao H, Fernandes V, Kalyanaraman B, et al. Impact of pulmonary arterial endothelial cells on duroquinone redox status. Free Radic Biol Med. 2004; 37:86–103. [PubMed: 15183197]
32. Circu ML, Maloney RE, Aw TY. Disruption of pyridine nucleotide redox status during oxidative challenge at normal and low glucose states: Implications for cellular ATP, mitochondrial respiratory activity and reducing capacity in colon epithelial cells. Antioxidants and Redox Signalling. 2011 In Press.
33. Stubberfield CR, Cohen GM. Interconversion of NAD(H) to NADP(H). A cellular response to quinone-induced oxidative stress in isolated hepatocytes. Biochem Pharmacol. 1989; 38:2631–7. [PubMed: 2764986]
34. Singh R, Lemire J, Mailloux RJ, Appanna VD. A novel strategy involved in [corrected] anti-oxidative defense: the conversion of NADH into NADPH by a metabolic network. PLoS ONE. 2008; 3:e2682. [PubMed: 18628998]
35. Audi SH, Merker MP, Krenz GS, Ahuja T, Roerig DL, Bongard RD. Coenzyme Q_1redox metabolism during passage through the rat pulmonary circulation and the effect of hyperoxia. J Appl Physiol. 2008; 105:1114–26. [PubMed: 18703762]
36. Angeloni C, Leoncini E, Malaguti M, Angelini S, Hrelia P, Hrelia S. Modulation of phase II enzymes by sulforaphane: implications for its cardioprotective potential. J Agric Food Chem. 2009; 57:5615–22. [PubMed: 19456137]
37. Cho HY, Imani F, Miller-DeGraff L, Walters D, Melendi GA, Yamamoto M, et al. Antiviral activity of Nrf2 in a murine model of respiratory syncytial virus disease. Am J Respir Crit Care Med. 2009; 179:138–50. [PubMed: 18931336]

38. Hanlon N, Coldham N, Sauer MJ, Ioannides C. Modulation of rat pulmonary carcinogen-metabolising enzyme systems by the isothiocyanates erucin and sulforaphane. Chem Biol Interact. 2009; 177:115–20. [PubMed: 18823965]
39. Riedl MA, Saxon A, Diaz-Sanchez D. Oral sulforaphane increases Phase II antioxidant enzymes in the human upper airway. Clinical Immunology. 2009; 130:244–51. [PubMed: 19028145]
40. Xue M, Qian Q, Adaikalakoteswari A, Rabbani N, Babaei-Jadidi R, Thornalley PJ. Activation of NF-E2-related factor-2 reverses biochemical dysfunction of endothelial cells induced by hyperglycemia linked to vascular disease. Diabetes. 2008; 57:2809–17. [PubMed: 18633117]
41. Malhotra D, Thimmulappa R, Navas-Acien A, Sandford A, Elliott M, Singh A, et al. Decline in NRF2-regulated antioxidants in chronic obstructive pulmonary disease lungs due to loss of its positive regulator, DJ-1. Am J Respir Crit Care Med. 2008; 178:592–604. [PubMed: 18556627]
42. Clarke JD, Dashwood RH, Ho E. Multi-targeted prevention of cancer by sulforaphane. Cancer Lett. 2008; 269:291–304. [PubMed: 18504070]
43. Ahn YH, Hwang Y, Liu H, Wang XJ, Zhang Y, Stephenson KK, et al. Electrophilic tuning of the chemoprotective natural product sulforaphane. PNAS. 2010; 107:9590–5. [PubMed: 20439747]
44. Asakage M, Tsuno NH, Kitayama J, Tsuchiya T, Yoneyama S, Yamada J, et al. Sulforaphane induces inhibition of human umbilical vein endothelial cells proliferation by apoptosis. Angiogenesis. 2006; 9:83–91. [PubMed: 16821112]
45. Bertl E, Bartsch H, Gerhauser C. Inhibition of angiogenesis and endothelial cell functions are novel sulforaphane-mediated mechanisms in chemoprevention. Mol Cancer Ther. 2006; 5:575–85. [PubMed: 16546971]
46. Crane MS, Howie AF, Arthur JR, Nicol F, Crosley LK, Beckett GJ. Modulation of thioredoxin reductase-2 expression in EAhy926 cells: Implications for endothelial selenoprotein hierarchy. Biochimica et Biophysica Acta - General Subjects. 2009; 1790:1191–7.
47. Chen XL, Dodd G, Kunsch C. Sulforaphane inhibits TNF-alpha-induced activation of p38 MAP kinase and VCAM-1 and MCP-1 expression in endothelial cells. Inflamm Res. 2009; 58:513–21. [PubMed: 19277846]
48. Shan Y, Zhao R, Geng W, Lin N, Wang X, Du X, et al. Protective effect of sulforaphane on human vascular endothelial cells against lipopolysaccharide-induced inflammatory damage. Cardiovasc Toxicol. 2010; 10:139–45. [PubMed: 20405237]
49. Tan XL, Shi M, Tang H, Han W, Spivack SD. Candidate dietary phytochemicals modulate expression of phase II enzymes GSTP1 and NQO1 in human lung cells. Journal of Nutrition. 2010; 140:1404–10. [PubMed: 20554899]
50. Tome ME, Johnson DB, Samulitis BK, Dorr RT, Briehl MM. Glucose 6-phosphate dehydrogenase overexpression models glucose deprivation and sensitizes lymphoma cells to apoptosis. Antioxid Redox Signal. 2006; 8:1315–27. [PubMed: 16910779]
51. Hartwick AT, Sivak JG. Epithelial activity of hexokinase and glucose-6-phosphate dehydrogenase in cultured bovine lenses recovering from pharmaceutical-induced optical damage. Mol Vis. 2003; 9:594–600. [PubMed: 14627957]
52. Dobrina A, Patriarca P. Neutrophil-endothelial cell interaction. Evidence for and mechanisms of the self-protection of bovine microvascular endothelial cells from hydrogen peroxide-induced oxidative stress. J Clin Invest. 1986; 78:462–71. [PubMed: 3734101]
53. Asahina T, Kashiwagi A, Nishio Y, Ikebuchi M, Harada N, Tanaka Y, et al. Impaired activation of glucose oxidation and NADPH supply in human endothelial cells exposed to H_2O_2in high-glucose medium. Diabetes. 1995; 44:520–6. [PubMed: 7729609]
54. Ernster L, Danielson L, Ljunggren M. DT diaphorase. I. Purification from the soluble fraction of rat-liver cytoplasm, and properties. Biochim Biophys Acta. 1962; 58:171–88. [PubMed: 13890666]
55. Whitesell RR, Ward M, McCall AL, Granner DK, May JM. Coupled glucose transport and metabolism in cultured neuronal cells: determination of the rate-limiting step. J Cereb Blood Flow Metab. 1995; 15:814–26. [PubMed: 7673374]
56. Kirkman HN, Gaetani GF, Clemons EH. NADP-binding proteins causing reduced availability and sigmoid release of $NADP^+$in human erythrocytes. Journal of Biological Chemistry. 1986; 261:4039–45. [PubMed: 3949801]

57. Sies, H. Nicotinamide Nucleotide Compartmentation. In: Sies, H., editor. Metabolic Compartmentation. London: Academic Press; 1982. p. 205-31.
58. Hinshaw DB, Burger JM. Protective effect of glutamine on endothelial cell ATP in oxidant injury. J Surg Res. 1990; 49:222–7. [PubMed: 2395368]
59. Radovits T, Zotkina J, Lin LN, Bömicke T, Arif R, Gerö D, Horváth EM, Karck M, Szabó C, Szabó G. Poly(ADP-ribose) polymerase inhibition improves endothelial dysfunction induced by reactive oxidant hydrogen peroxide in vitro. Eur J Pharmacol. 2007; 564:158–66. [PubMed: 17397824]
60. Coyle C, Martinez L, Coleman M, Spitz D, Weintraub N, Kader K. Mechanisms of H_2O_2-induced oxidative stress in endothelial cells. Free Radic Biol Med. 2006; 40:2206–13. [PubMed: 16785034]
61. Leopold JA, Walker J, Scribner AW, Voetsch B, Zhang YY, Loscalzo AJ, et al. Glucose-6-phosphate dehydrogenase modulates vascular endothelial growth factor-mediated angiogenesis. J Biol Chem. 2003; 278:32100–6. [PubMed: 12777375]
62. Salvemini F, Franze A, Iervolino A, Filosa S, Salzano S, Ursini MV. Enhanced glutathione levels and oxidoresistance mediated by increased glucose-6-phosphate dehydrogenase expression. J Biol Chem. 1999; 274:2750–7. [PubMed: 9915806]
63. Leopold JA, Zhang YY, Scribner AW, Stanton RC, Loscalzo J. Glucose-6-phosphate dehydrogenase overexpression decreases endothelial cell oxidant stress and increases bioavailable nitric oxide. Arterioscler Thromb Vasc Biol. 2003; 23:411–7. [PubMed: 12615686]
64. Kuo WY, Tang TK. Effects of G6PD overexpression in NIH3T3 cells treated with tert-butyl hydroperoxide or paraquat. Free Radic Biol Med. 1998; 24:1130–8. [PubMed: 9626567]
65. Gumaa KA, McLean P. The pentose phosphate pathway of glucose metabolism. Enzyme profiles and transient and steady-state content of intermediates of alternative pathways of glucose metabolism in Krebs ascites cells. Biochem J. 1969; 115:1009–29. [PubMed: 5360673]
66. Wasserman DH, Kang L, Ayala JE, Fueger PT, Lee-Young RS. The physiological regulation of glucose flux into muscle in vivo. J Exp Biol. 2011; 214:254–62. [PubMed: 21177945]
67. Gasper AV, Al Janobi A, Smith JA, Bacon JR, Fortun P, Atherton C, et al. Glutathione S-transferase M1 polymorphism and metabolism of sulforaphane from standard and high-glucosinolate broccoli. Am J Clin Nutr. 2005; 82:1283–91. [PubMed: 16332662]
68. Hu R, Hebbar V, Kim BR, Chen C, Winnik B, Buckley B, et al. In vivo pharmacokinetics and regulation of gene expression profiles by isothiocyanate sulforaphane in the rat. J Pharmacol Exp Ther. 2004; 310:263–71. [PubMed: 14988420]

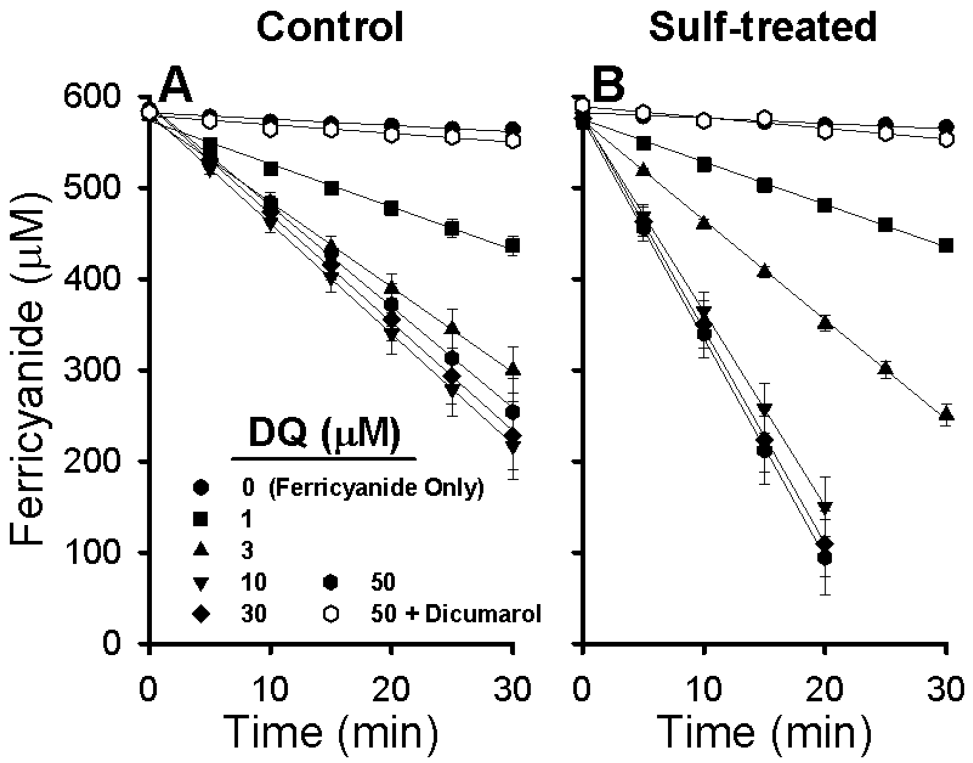

Figure 1. NQO1 activity in intact control and sulf-treated cells measured in the extracellular medium as DQ-mediated ferricyanide reduction

The figure shows the ferricyanide concentration versus time progress curves following addition of ferricyanide (600 μM) with DQ (1 - 50 μM) to the control (A) or sulf-treated (B) cells. The effect of the competitive NQO1 inhibitor dicumarol (10 μM) at 50 μM DQ is shown in (A) and (B). Also shown in (A) and (B) is the ferricyanide only data (without DQ). The latter was subtracted as background from data obtained in the presence of DQ. For the experiments without inhibitors, the symbols represent the data from 12 paired control and sulf-treated cell experiments at 6 DQ concentrations, for which the cell proteins (mean ± SEM in mg) were 1.19 + 0.03 (n = 72) and 1.00 ± 0.04 (n = 72), respectively ($p < 0.05$, t-test); cell proteins for dicumarol studies were 1.49 and 1.32 (n = 1 each) in (A) and (B) respectively. The solid lines represent linear regression fits to the data. The % LDH release measured at the end of each experiment did not exceed 1.58 ± 0.37% of total cell LDH for all the studies combined, with no significant differences between conditions ($p>0.05$, ANOVA).

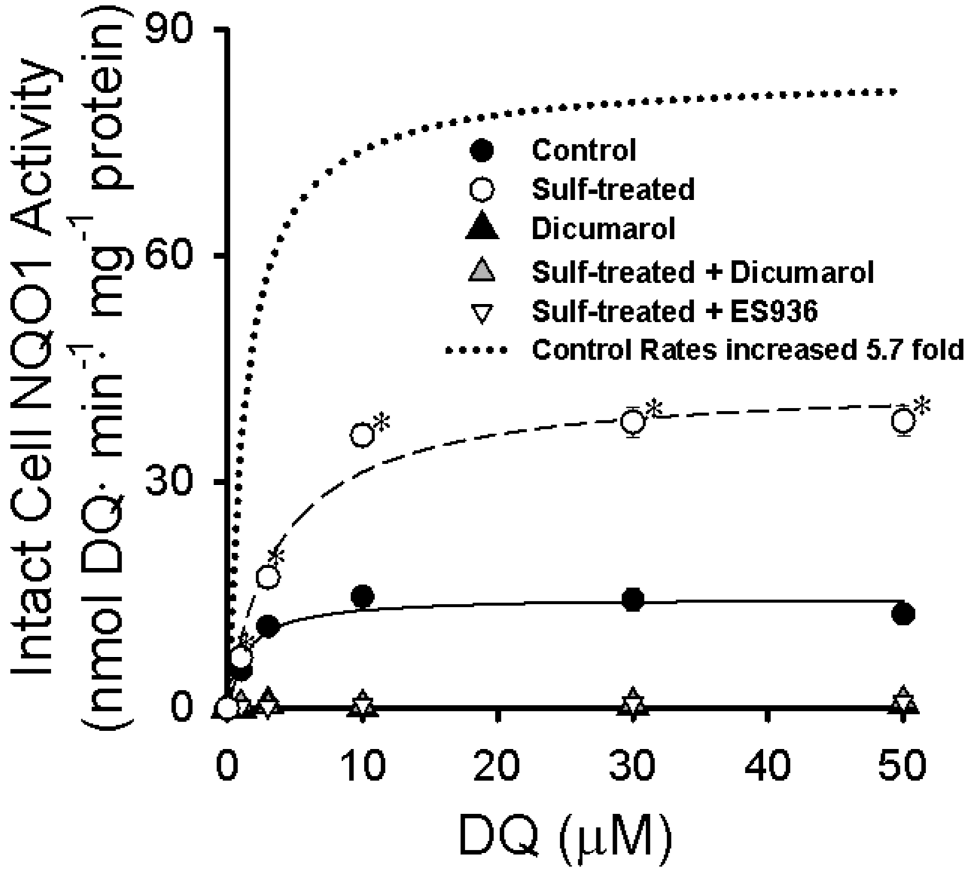

Figure 2. Effect of DQ concentration on NQO1 activity in intact control and sulf-treated cells

The symbols represent the DQ reduction rates, calculated as described in the Methods from the data in Figure 1, giving the intact cell NQO1 activities. Also shown are control and sulf-treated cell DQ reduction rates at 1 – 50 μM DQ with dicumarol (10 μM) and the sulf-treated cell DQ reduction rates at 1 – 50 μM DQ with ES936 (0.5 μM). The symbols represent the mean ± SEM for n = 12 determinations each for control and sulf-treated cells, and n = 1 each for dicumarol and ES936 conditions at each DQ concentration. The solid and dashed lines are Michaelas-Menten fits to the data and the dotted line represents 5.7 times the control activity across the full range of DQ concentrations. The control and sulf-treated cell proteins are as in Figure 1, proteins for control and sulf-treated cells with dicumarol (n = 6 each) were 1.37 ± 0.06 and 1.41 ± 0.03, respectively, and for sulf-treated cells with ES936 (n=6), 1.03 ± 0.03. *Means are significantly different than control at the same DQ concentration ($p<0.05$; t-test).

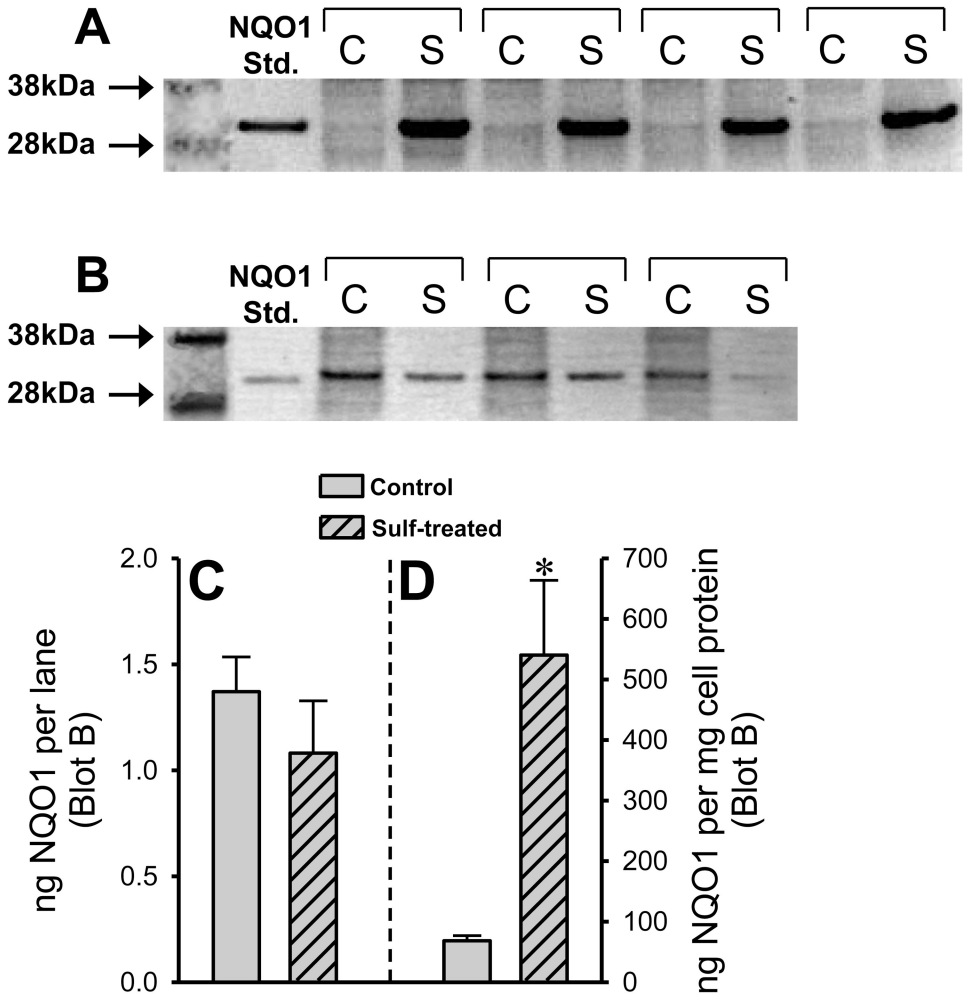

Figure 3. Immunoblots of control and sulf-treated cell NQO1

(A) Blot in which equivalent amounts of cell lysate (20 μg protein) were loaded onto each lane, from 4 sets of control (C) and sulf-treated (S) cell cultures, wherein the individual sets are from the 4 different cell populations. (B) Blot in which 10 times more control (20 μg) than sulf-treated (2 μg) cell lysate protein was loaded onto each lane for 3 sets of control and sulf-treated cell cultures, where the sets are from different populations. Human recombinant NQO1 was the standard in both (A) and (B). (C) Total ng NQO1 protein (mean ± SEM) in the control and sulf-treated cell lysates calculated from the lane intensities in blot (B). The NQO1 standard was used for calibration as described in the Methods. (D) NQO1 protein per mg cell lysate protein (mean ± SEM) calculated from the lane intensities in (B). *Significantly different than control ($p<0.05$, t-test).

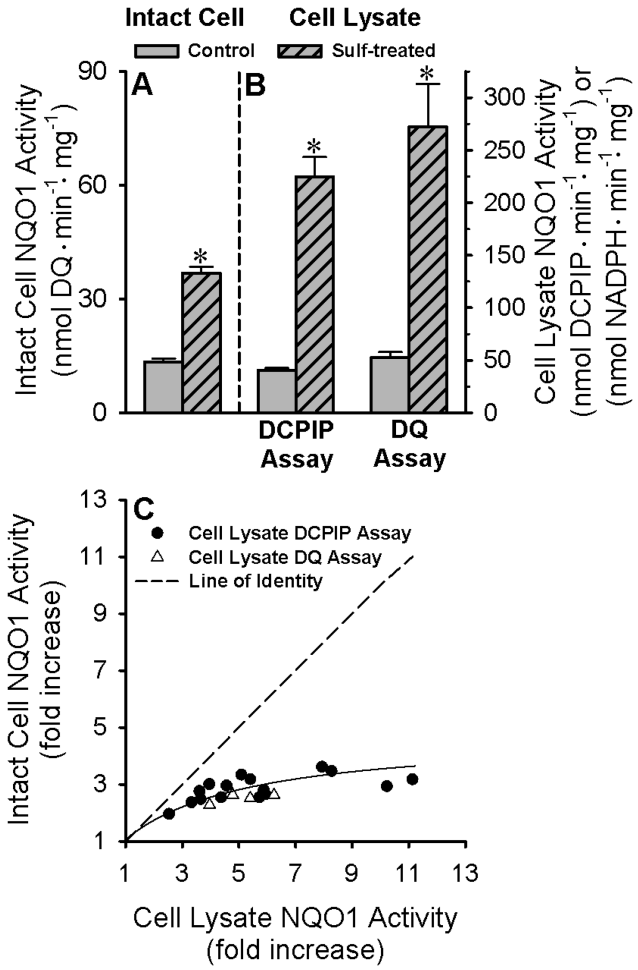

Figure 4. Relationship between the sulforaphane-induced increase in intact cell and cell lysate NQO1 activities

(A) Maximal intact cell NQO1 activity (means ± SEM) of control and sulf-treated cells (n = 16 pairs control and sulf-treated cells, including all the Figure 1 data), studied at 50 μM DQ. (B) Cell lysate NQO1 activity (means ± SEM) using DCPIP or DQ as the electron acceptor in n = 16 or n = 4 pairs, respectively, of control and sulf-treated cells, with each pair derived from the same passage studied in parallel on the same day. (C) The fold increase in intact cell NQO1 activity, taken from (A) plotted vs the fold difference in cell lysate NQO1 activity, taken from (B), wherein the cell lysate data was obtained using either the DCPIP (closed circles) or the DQ (open triangles) as the electron acceptor. The dashed line is the line of identity, that is, the expected relationship if the intact cell activity rose in proportion to cell lysate activity. *Significantly different than matched controls ($p < 0.05$, t-test).

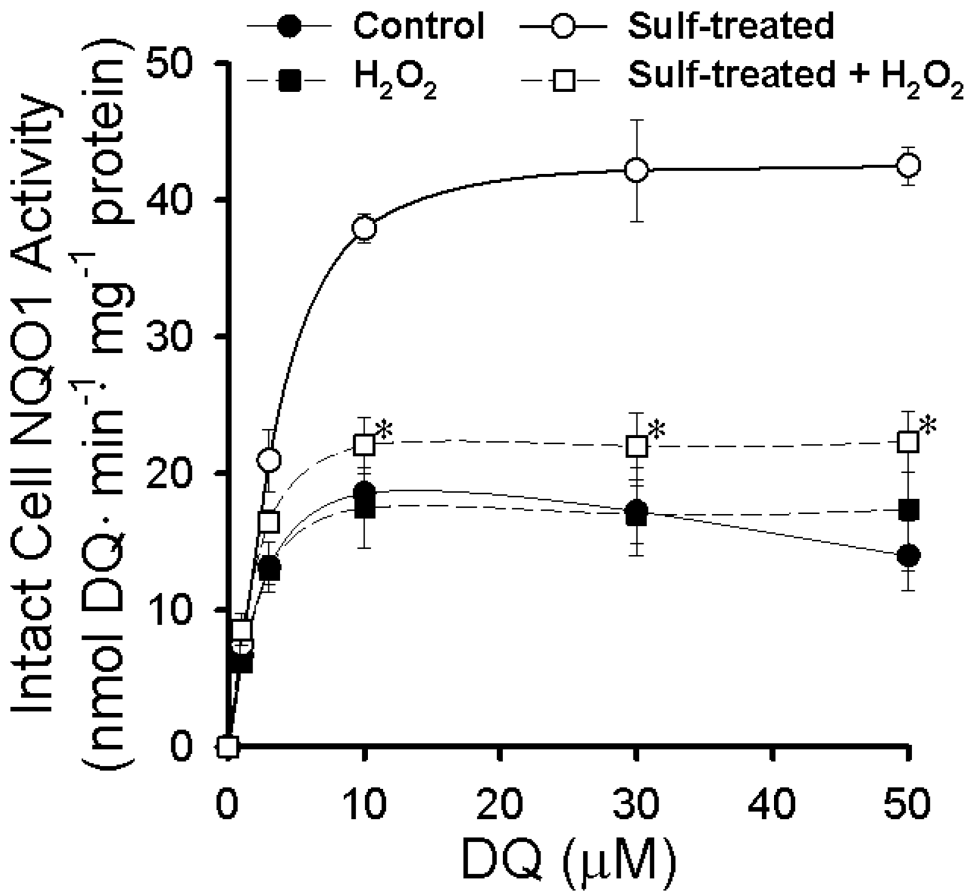

Figure 5. H_2O_2depresses maximum intact NQO1 activity in sulf-treated but not control cells

H_2O_2 (1 mM) was added to the cell medium 10 minutes prior to addition of DQ and ferricyanide, and was also present throughout the 30 min period for measuring intact cell NQO1 activity using the approach described in Figures 1 and 2. The symbols represent the mean ± SEM from n=3 experiments for each of the 4 conditions. The cell proteins (mean ± SEM, in mg) were as follows: control (1.03 ± 0.05), H_2O_2 (1.00 ± 0.04), sulf-treated (0.69 ± 0.03), sulf-treated + H_2O_2 (0. 70 ± 0.04). *Significantly different than sulforaphane-treated ($p<0.05$, t-test).

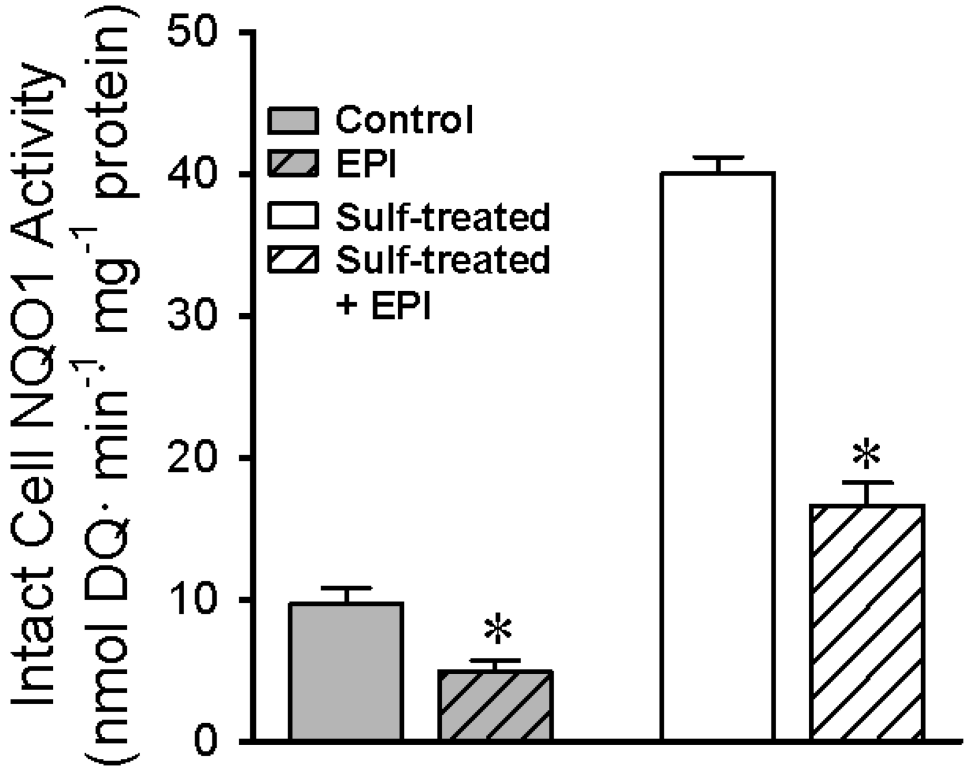

Figure 6. G-6-PDH inhibitor epiandrosterone (EPI) partially blocks NQO1 activity in intact control and sulf-treated cells

Intact control and sulforaphane cell NQO1 activities were measured in the absence or presence of EPI (30 μM). The bars represent the mean ± SEM for n=4 determinations for the control ± EPI and n=5 for the sulf-treated cells ± EPI. LDH release for the control cells was 1.6 ± 0.17% and 2.14 ± 0.33% in the absence and presence of EPI, respectively ($p>0.05$, t-test); LDH release for the sulf-treated cells was 1.25 ± 0.05% and 2.6 ± 0.17% in the absence and presence of EPI, respectively ($p<0.05$; t-test). The cell proteins (mean ± SEM, in mg) for the controls ± EPI were 1.52 ± 0.03 mg and for the sulf-treated cells were 1.06 ± 0.10 mg). *Significantly different than without EPI ($p<0.05$, t-test).

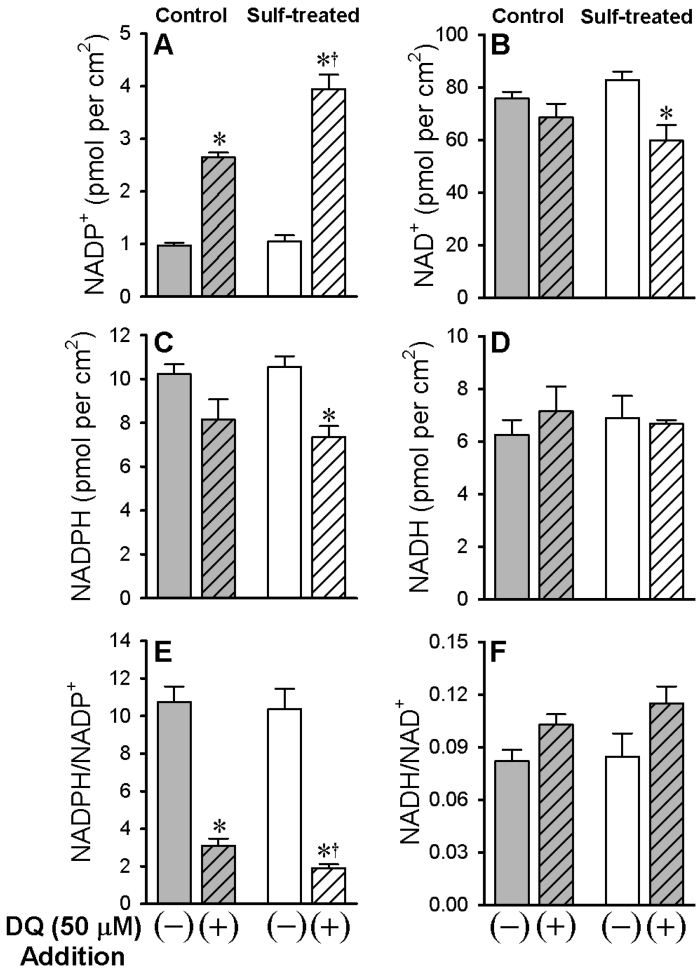

Figure 7. Impact of intact cell NQO1 activity on intracellular pyridine nucleotides in control and sulf-treated cells

Fifteen min prior to KOH extraction for HPLC, cells were incubated in medium without (-) or with (+) DQ (50 μM), the latter to elicit maximal intact cell NQO1 activity. Bars represent means ± SEM of n=7 control without DQ and n=4 each for the other conditions. *Significantly different than without DQ; † significantly different than control with DQ ($p<0.05$; ANOVA and Tukey test for multiple pairwise comparisons).

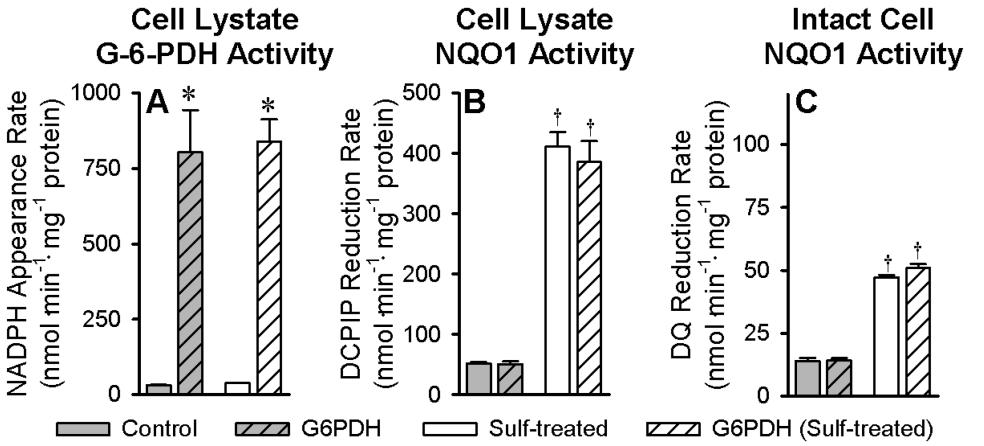

Figure 8. G-6-PDH gene overexpression increases G-6-PDH activity but is insufficient to increase intact cell NQO1 activity in sulf-treated cells

Effect of G-6-PDH gene overexpression (G6PDH) on cell lysate (A) G-6-PDH and (B) NQO1 activities and on (C) intact cell NQO1 activities in control (mock transfected) and sulf-treated cells. Bars represent mean ± SEM for n=5 for each condition. LDH release was not significantly different for the different conditions, and the mean ± SEM for the combined data was 2.53 ± 0.21 %. The cell proteins for the control, G6PDH, Sulf-treated and G6PDH + Sulf-treated conditions were 1.52 ± 0.11, 1.36 ± 0.09, 0.96 ± 0.12 and 1.02 ± 0.12 (mean ± SEM) mg, respectively. (A) *Significantly different than without overexpression; (B) and (C) †significantly different than controls or G6PDH without sulforaphane (ANOVA; $p<0.05$, Tukey test).

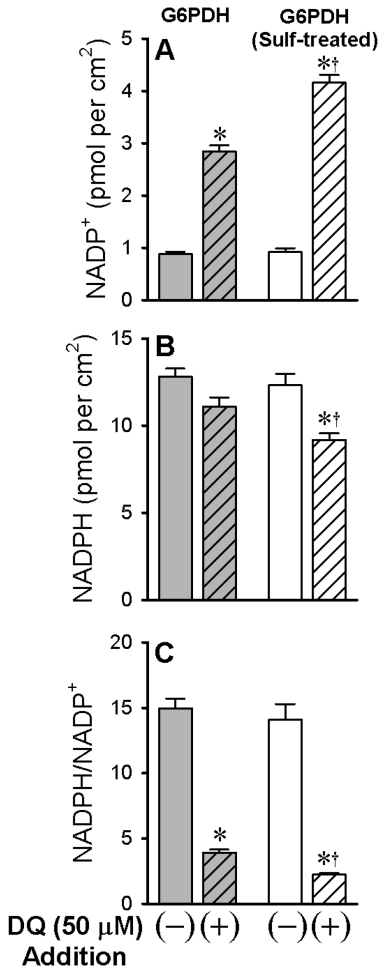

Figure 9. G-6-PDH gene overexpression does not alter pyridine nucleotide responses to NQO1 activation in either control or sulf-treated cells

Fifteen min prior to KOH extraction for HPLC, cells were incubated in medium without (-) or with (+) DQ (50 μM), the latter to elicit maximal intact cell NQO1 activity. Bars represent means ± SEM of n=13 for G-6-PDH overexpression (G6PDH) without DQ and n=10 each for the other conditions. *Significantly different than without DQ; † significantly different than G6PDH with DQ; ($p<0.05$; ANOVA and Tukey test for multiple pairwise comparisons).

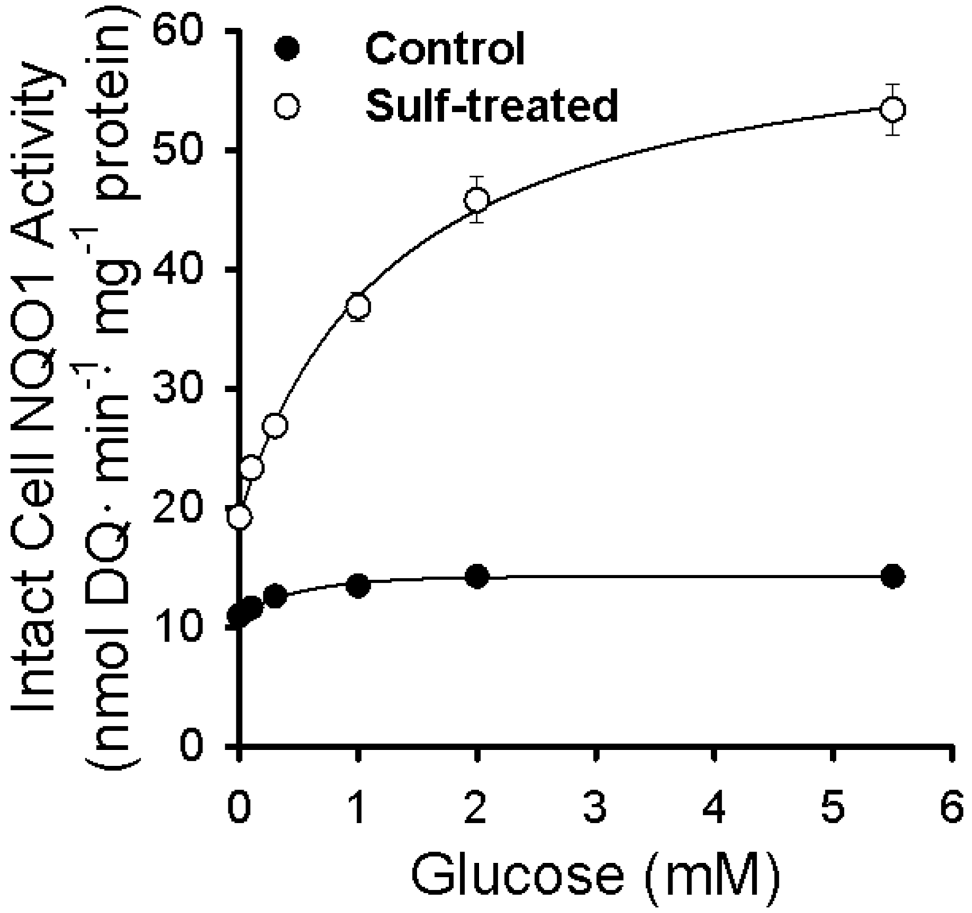

Figure 10. Increased sensitivity of sulf-treated cell NQO1 activity to limiting the extracellular glucose concentration

Symbols represent mean ± SEM for 4 determinations for each condition. There was no statistical difference ($p > 0.05$; t-test) between the %LDH release or protein for the control and sulforaphane cells in the absence of glucose or at any glucose concentration studied. The mean ± SEM for all 48 samples for % LDH release was 1.46 ± 0.11% and the protein was 1.20 ± 0.02 mg.